Sensors and Actuators B 234 (2016) 53–62

Contents lists available at ScienceDirect

Sensors and Actuators B: Chemical

journal homepage: www.elsevier.com/locate/snb

Smart valve: Polymer actuator to moisture soil control

Marcelo R. Romero*, Alexis Wolfel, Cecilia I. Alvarez Igarzabal

IMBIV-CONICET, Departamento de Química Orgánica, Facultad de Ciencias Químicas, Universidad Nacional de Córdoba, Haya de la Torre y Medina Allende, Edificio de Ciencias II, Ciudad Universitaria, Córdoba X5000HUA, Argentina

ARTICLE INFO

Article history:
Received 29 December 2015
Received in revised form 8 April 2016
Accepted 17 April 2016
Available online 26 April 2016

Keywords:
Hydrogel
Smart valve
Irrigation
Polymer actuator
Soil moisture

ABSTRACT

The adequate use of water for irrigation in agriculture is a widespread concern. In this study, we developed an autonomous smart system consisting of a new hydrogel into a valve, which regulates the flow of water according to soil moisture. The main objective was to find an alternative to avoid waste of water. Yet, hydrogel development and study of the quantitative relationship between its properties and soil moisture were also important to achieve this aim. The hydrogel was synthesized from tris[(hydroxymethyl) methyl]acrylamide (NAT) copolymerized with methyl methacrylate (MMA) and crosslinked with *N,N′*-methylene bis(acrylamide) (BIS). The use of cellulose (2% w/v) avoids hydrogel breakage during swelling-deswelling. The relation between swelling ratio, force of expansion and moisture was evaluated for the novel hydrogel. It was found that as soil moisture increases, the gel swells, while expansion force diminishes. These properties showed linear relationship in the range studied. The three-dimensional network formed by flexible chains has the attribute of exerting a great force when it expands (≅15 N for a hydrogel disc of 1 cm^2). When the material was put in contact with the ground, it swelled and deswelled without breaking. The hydrogel within the valve was able to open and close the passage of water. The valve prototype was tested during four months with a plant. During this period, only three liters of irrigation water were used monthly, instead of about half a liter daily. Hence, an autonomous actuator capable of controlling soil moisture was developed based on a new hydrogel.

1. Introduction

Water demand should be reduced by increasing the efficient use of this resource [1]. One way to reduce water consumption is by developing efficient irrigation systems [2]. The use of new technologies should be aimed to adjust the irrigation to the needs of the plant [3]. Many published works have been aimed to the development of systems with controlled irrigation, using actuators that operate according to the soil moisture. Mainly, they are made of electronic sensors coupled to actuators that operate using wires or batteries [4–7]. Hence, high costs and contamination of the batteries, the energy demand and the computational management are the major problems of these systems [8–11]. Chemical actuators can be considered as possible smart irrigation systems because they use energy for chemical changes in their environment and transform it into a mechanical response [12]. These chemo-mechanical transducers are not dependent upon external power sources, enabling their use in places where other devices are particularly limited [12]. Different types of actuators capable of activating mechanisms such as valves [13], pumps [14] and mixers have been developed [15]. Hydrogels are used as chemical actuators because they can reversibly swell in response to chemical or physical changes in the environment. Therefore, they are being studied for applications such as sensors [16], artificial muscles [17] and as components in miniaturized devices called “lab on a chip” [18].

The development of hydrogels based actuators requires to know the swelling behavior and mechanical properties of the material [19].

Hydrogels can swell in water increasing their volume many times. Taking advantage of this property, acrylamide-containing hydrogels have been used to increase moisture retention in soils [20]. However, the evaluation of the water sensitivity of these types of material is necessary to develop actuators. The swelling equilibrium reflects the sensitivity to moisture changes.

The composition of each hydrogel may show a particular reversible degree in swelling/deswelling cycles [21]. In this sense, the incorporation of fibers or particles into polymer networks has been reported to improve their mechanical properties [22]. In addition, materials that incorporate cellulose have shown excellent results [23,24].

The elasticity in hydrogels can be regulated by controlling the hydrophilicity of the polymer network [25]. To accomplish this task,

* Corresponding author.
E-mail address: marceloricardoromero@gmail.com (M.R. Romero).

http://dx.doi.org/10.1016/j.snb.2016.04.104
0925-4005/

methyl methacrylate (MMA) has been used in combination with other more polar monomers [26]. The control of composition of hydrogel will allow controlling hydrophobicity and regulating the interactions between the chains and water, the wetting capacity and therefore the maximum degree of swelling of the hydrogel. The designed material should also minimize the dependence of the system upon other stimuli such as pH, ionic strength and temperature. Previously, we developed a hydrogel, a pH-dependent actuator, using tris[(hydroxymethyl) methyl]acrylamide (NAT) and itaconic acid as co-monomers [27].

In this work, we present the development of a new hydrogel that can actuate independently of soil acidity. Therefore, to yield a material which serves the purposes of this study, NAT and MMA monomers were used. The hydrogel should act as a moisture sensor and control the flow in an auto-regulated form. In this research, various studies were conducted to know the behavior of the gels in contact with the ground at different moisture levels and to determine the ability of the network to generate enough normal force (NF) to operate the valve during swelling.

Furthermore, the selected hydrogel was incorporated in a mechanical system that controls water flow according to the swelling of the gel, this property being associated with the water amount present in the ground. Since the hydrogel is in equilibrium with soil moisture, it shrinks when humidity decreases, allowing the opening of the valve and passage of water, whereas the hydrogel expands and closes the flow of water when moisture is high enough.

The applicability of the system was evaluated with a prototype valve to control soil humidity by placing the device in a potted plant (White calla lily) [28] for more than 100 days.

2. Materials and methods

2.1. Reagents

The following reagents were used as received: tris [(hydroxymethyl) methyl] acrylamide (NAT) (Sigma); methyl methacrylate (MMA) (Sigma); *N*,*N*′-methylene bis(acrylamide) (BIS) (Sigma); (+)-*N*,*N*′-diallyltartramide (DAT)(Sigma); *N*,*N*,*N*′,*N*′-tetramethyethylenediamine (TEMED) (Sigma); ammonium persulfate (APS) (Anhedra); native fibrous cellulose powder MN300HR (Macherey, Nagel & Co., fiber length (95%) 2–20 μm, average degree of polymerization 400–500, specific surface according to Blaine 15000 cm^2/g), *n*-heptane (Dorwill); ethanol absolute (Sintorgan) and porous stone HMA-547 (Gilson Company Inc.). The solutions were prepared with ultrapure water (18 MΩ cm^{-1}).

2.2. Synthesis and characterization of the hydrogels

2.2.1. Synthesis

The hydrogels were prepared by free radical polymerization. A mixture of water/ethanol (60:40) was used for the reactions. As shown in Table 1, cellulose powder was added to 5 mL of the mixture water/ethanol and sonicated for 10 min at mid intensity (≅40 WL^{-1}, 40 kHz, Ultrasonic Cleaner model Power Sonic 410, Hwashin Technology). The NAT/MMA molar ratio was varied as shown in Table 1 (total monomer concentration of 1.4 M; [NAT] + [MMA] = 1.4 M), the crosslinking agent (BIS or DAT, 5–10% with respect to 1.4 M) and APS (3.7–7.4% with respect to 1.4 M) were dissolved in the cellulose/water/ethanol mixture using a vial with a rubber cap. The solution was cooled on an ice bath and deoxygenated with N_2 for 10 min. To initiate polymerization, 0.5 mL of an aqueous TEMED solution (0.32 M) was added to the vial and the whole solution was transferred to a plastic syringe of 5 mL. The syringe was placed in a water bath at 37 °C for 16 or 40 h as shown in Table 1. Finally, the hydrogels were cut into discs of 3 mm thick and 12 mm in diameter and washed thoroughly with water. Products p(MMA-NAT) 1–12 were yielded. All the syntheses were performed in triplicate.

2.2.2. Optical microscopy and scanning electron microscopy (SEM)

The surface morphology of hydrogel samples was analyzed by optical microscopy using a digital microscope Nisuta NS-DIMI USB. The optical analysis was carried out using samples dried in an oven at 37 °C until constant weight.

The scanning electron microscopy (SEM) was performed using a Σigma FE-SEM from the Electron Microscopy Laboratory (LAMARX), FAMAF, Universidad Nacional de Córdoba, Córdoba, Argentina. SEM studies were performed with freeze-dried samples after swelling in water and sputter-coated with platinum (Pt).

2.2.3. Study of swelling at equilibrium

The samples were dried in an oven at 37 °C until constant weight. The dehydrated hydrogel discs were placed in water and swollen for 3 days until constant weight at 25 °C. When the equilibrium mass was obtained, equilibrium swelling ratio as percentage (%ESR) was calculated according to Eq. (1):

$$\%\mathrm{ESR} = \frac{[m_e - m_d]}{m_d \times 100} \quad (1)$$

where m_e is the mass of the sample at swelling equilibrium and m_d is the dried mass. The hydrogel was weighted using a Mettler Toledo balance (New classic MF, model MS204S; 0.1 mg precision).

2.2.4. Swelling kinetics of hydrogels and diffusion rate of water

The swelling kinetics of the hydrogels was studied by determining swelling rate (SR) at different times. SR was calculated using Eq. (2), where m_t is the mass of the sample at a given time:

$$\mathrm{SR} = \frac{[m_t - m_d]}{m_d} \quad (2)$$

Dried hydrogel discs were placed in water to swell; the change in weight was recorded as a function of time, until reaching constant mass. The hydrogel was weighted using a Mettler Toledo balance (New classic MF, model MS204S; 0.1 mg precision). All assays were performed in triplicate. On the basis of the swelling kinetics (S), the type of diffusion of water into the samples was estimated using Eq. (3) [29]

$$\mathrm{S} = \frac{M_t}{M_\infty} = kt^m \quad (3)$$

where M_t is the mass of water into the sample at time t, M_∞ is the mass of water into the sample at equilibrium and k is a constant related to the network structure. The exponent m is a number related to diffusion type. This equation is applicable to swelling lower than 60% of equilibrium swelling. The value of m and k was obtained from the slope and the intercept of the curve *ln* S vs. *ln t*, respectively.

2.2.5. Contact angle measurements

Contact angle measurements were performed by the Sessile Drop method using a homemade contact angle goniometer. Deionized water drops were used over dried hydrogel discs. All assays were performed with water drops of (4.00 ± 0.04) mm^3 measured with an automatic pipette of the contact angle goniometer. The water drop was dropped from a distance of (2.00 ± 001) mm from the flat surface of the sample. Before and after that the drop touched the surface, a video was recorded using a camera CMOS at 15 frames per second. The size of the images captured was of 640 × 480 pixels and the video was in avi format. Each video was processed

Table 1
Hydrogels composition.

Synthesis	Co-monomers (molar ratio)	Cellulose powder w/v (%)	Crosslinking agent	APS (%)	Reaction time (h)
p (MMA-NAT)1	MMA:NAT (50:50)	0	DAT 5%	3.7	16
p (MMA-NAT)2	MMA:NAT (50:50)	0	DAT 5%	3.7	40
p (MMA-NAT)3	MMA:NAT (50:50)	0	DAT 5%	7.4	16
p (MMA-NAT)4	MMA:NAT (50:50)	0	DAT 10%	3.7	16
p (MMA-NAT)5	MMA:NAT (50:50)	0	DAT 10%	7.4	16
p (MMA-NAT)6	MMA:NAT (50:50)	0	DAT 10%	7.4	40
p (MMA-NAT)7	MMA:NAT (20:80)	0	DAT 5%	3.7	16
p (MMA-NAT)8	MMA:NAT (20:80)	0	BIS 5%	3.7	16
p (MMA-NAT)9	MMA:NAT (20:80)	0.4	BIS 5%	3.7	16
p (MMA-NAT)10	MMA:NAT (20:80)	0.8	BIS 5%	3.7	16
p (MMA-NAT)11	MMA:NAT (20:80)	2	BIS 5%	3.7	16
p (MMA-NAT)12	MMA:NAT (20:80)	10	BIS 5%	3.7	16

with SPANISH-DUB software and different frames were selected at 1,2,3,5,7,10 and 15 s in bmp format. Finally, the bmp images were converted to 8 bit grayscale with IMAGEJ 1.4 g software. The contact angle was measured processing the images with plug-in LB-ABSA (Low Bond Axisymmetric Drop Shape Analysis by Aurélien Stalder). The results obtained correspond to the contact angle by the method of subpixel. All assays were performed in triplicate at room temperature. Photos of the contact angle goniometer and an example of samples measured are available on Supporting information Figs. S1 and S2.

2.2.6. Studies of normal force (NF) kinetics

The NF produced by the hydrogel during hydration was recorded over time during 5 h. For this experiment, the dried hydrogel discs were cut on 7 mm diameter and 0.7 mm height. The sample was centrally placed between two plates of 25 mm diameter in the rheometer. Subsequently, water was placed between the plates until the remaining space was filled. The water produced the swelling of the hydrogel; we then measured the NF (N) caused by its expansion. The NF was detected by the capacitive probe inside of air bearing of a rheometer Anton Paar Physica MCR −301, with resolution of ±0.002 N and accuracy of 2.5% of measured value, ±0.03 N. During the determination, the space between the plates was kept constant. All tests were performed in quadruplicate at constant temperature (20.0 ± 0.1) °C. The scheme and a photo of the system to measure the NF are available on Supporting information Figs. S3 and S4.

2.2.7. ESR and NF of hydrogels previously equilibrated on soil with different moisture content

The hydrogels were previously equilibrated on soil, using potting soil as a model. To control the percentage of water present in the soil, it was initially dried in an oven at 105 °C for 4 h, until constant weight [22]. Furthermore, glass flasks of 100 mL were filled with 50 mL of dry soil and closed with a cap. Subsequently, different amounts of water were added to obtain 0, 15, 30, 45 and 60% v/v of soil moisture content. Each system was allowed to equilibrate for 48 h at 20 °C. Dried hydrogel discs were placed over the surface of different soil samples and equilibrated for a period of 5 days in the closed cup glass flasks.

After the period, ESR and NF were determined. ESR was calculated according to Eq. (1), with the mass of previously equilibrated hydrogel (m_e) and after being dried in an oven at 37 °C, until constant weight (m_d).

NF of the hydrogels previously equilibrated in soils with different moisture content was measured. For this, each hydrogel was placed between the plate of the balance Shimadzu Libror EB3200D and a fixed flat surface of glass. The last was placed parallel and close to the plate of the balance. The remaining space between the plate and the glass was filled with water. The NF produced by the hydrogel was registered as the mass change, until equilibrium, during 48 h. The results were normalized to hydrogels of 10 mm dry diameter. All experiments were performed in duplicate at room temperature. A scheme of the system is available on Supporting information Fig. S5.

2.2.8. Stability test for the hydrogels in soil

Dry hydrogel discs were weighted and put in soil containing 0, 15, 30, 40 and 60% v/v percentage of humidity, in a closed recipient. The hydrogels were left to swell freely for 3 months. After this period, the dry weight of each sample was determined again, and it was related to the original weight using the following ratio (Eq. (4)):

$$\frac{\left(m_f - m_i\right)}{m_i \times 100} \tag{4}$$

where m_f is the final mass after the period and m_i is the initial mass of the samples. All assays were performed in triplicate. Photos of the hydrated samples were also taken to compare their final morphologies.

2.3. Design and operational test of the actuator valve

2.3.1. Design of the valve

The valve consists of 4 mm height and 25 mm diameter and one of 2 mm height with the same diameter, screwed together (Fig. 1). For more details of design, see Supporting information (Figs S6–S9). The overhead disc contains a manual regulator for changing the height of the water inlet tube and thus control the opening and closing of the system. The regulator consists of a bronze screw of 1 cm height and 3.8 mm diameter, drilled longitudinally. The screw contains two nuts which are used to modify the height of the water inlet tube and lock the height, respectively. The inlet tube is a needle (Terumo® NEOLUS 21 G x 2″) which was blunt cut and is 10 mm long. The intermediate thick disc has a central hole and a side tube to conduct the fluid when the valve is open. Between the intermediate disk and the bottom one, a latex membrane of 100 μm thickness and 2.2 cm diameter was placed. The membrane prevents water filtration to the hydrogel directly before reaching the ground. The bottom thin disc has a hole in which a porous stone of 10 mm diameter was glued. This material is rigid but permeable to water. The stone has a hollow of 2 mm height and 4 mm diameter to hold within the hydrogel.

2.3.2. Operational stability test of the actuator

The operational stability was tested by placing the valve on the surface of soil in which a White calla lily was growing. The system was developed using the plant as probe for 4 months. To perform this assay, the plant and the valve were put inside a flowerpot with 10 L capacity. The water of the valve was supplied by

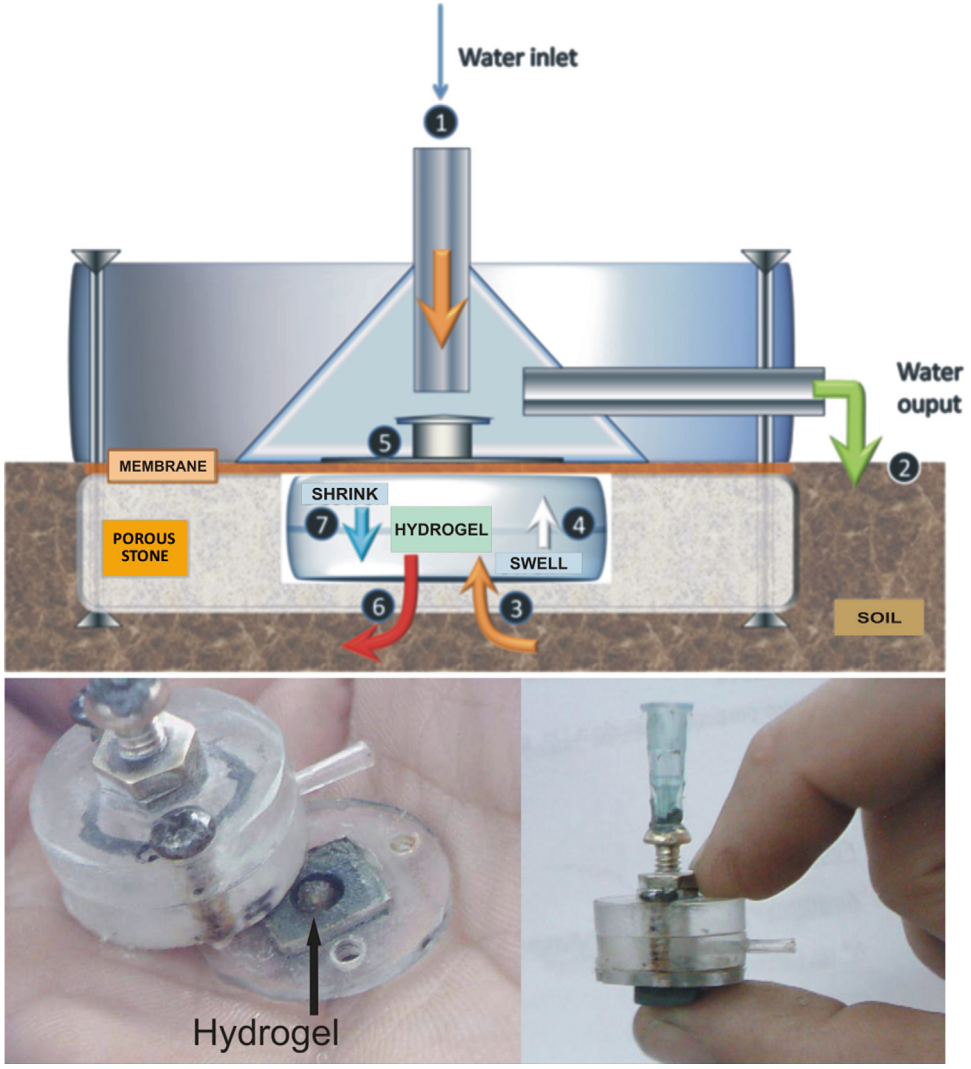

Fig. 1. (Top) Scheme of the valve prototype showing how the changes in volume of the hydrogel control the water flow across the system. (Bottom) Photos of valve prototype; (Left) The system was partially dissembled to show hydrogel p(MMA-NAT)11 inside the device (arrow). (Right) The photo shows the real dimensions of the system as compared with those of a hand.

a 5 L reservoir connected to a 1.6 mm internal diameter hose from Masterflex® (06409-14, Tygon® lab tubing). A 2 mm hole was made in the upper part of the reservoir to allow air interchange. The reservoir connected to the tube was then elevated to produce 2 m of water column [mH_2O] in the valve inlet. The hydrogel was previously hydrated with water for 24 h and then placed inside the prototype. The valve was connected to the tube and then placed on the surface of the soil next to the plant stem. The reservoir was refilled with water approximately once per month, without changing its position. Several photos were taken at different periods to reveal plant survival during valve operation.

3. Results and discussion

3.1. Analysis of synthesis products

Novel hydrogels were obtained by radical polymerization using 50:50 and 20:80 MMA-NAT ratio, as shown in Table 1. The relation between MMA and NAT was adjusted to obtain the optimal solubility of MMA to yield the final materials. The monomers at 50:50% molar ratios were solubilized in the solvent mixture. However, when the reaction started, a precipitate was observed before hydrogel formation, showing heterogeneity for [p(MMA-NAT) 1-6]. Moreover, products obtained from 20:80 MMA-NAT were homogeneous materials. Crosslinking agents such as DAT or BIS were evaluated; yet the hydrogels obtained with 5 or 10% DAT showed poor mechanical properties [p(MMA-NAT) 1-7]. These properties were slightly improved when 7.4% of APS was added instead of 3.7% or when the reaction time was increased from 16 to 40 h. However, p(MMA-NAT) 8 obtained with 20:80 MMA-NAT ratio, 5% BIS, 3.7% APS and 16 h of reaction time showed the best mechanical properties.

The p(MMA-NAT) 8 hydrogel was reproducible (the %ESR and NF measured for these materials exhibit a relative standard deviation close to 10%); nevertheless, when it was dried, the dehydrated material showed fractures. This effect could cause problems because the hydrogel in the actuator continuously switches from hydrated to dehydrated states. To solve this problem, cellulose fiber was chosen as a reinforcing reagent to improve the hydrogel properties. Cellulose fibers were added to p(MMA-NAT) 8 composition in different proportions (0.4, 0.8, 2, 5 and 10% w/v). When the cellulose fibers were added to the reaction mixture, hydrogels were obtained in all cases as products p(MMA-NAT) 9-12.

To analyze the effect of the presence of cellulose on the hydrogels, wettability and swelling properties were studied. Fig. 2A shows the contact angles of sessile drops of water after a contact

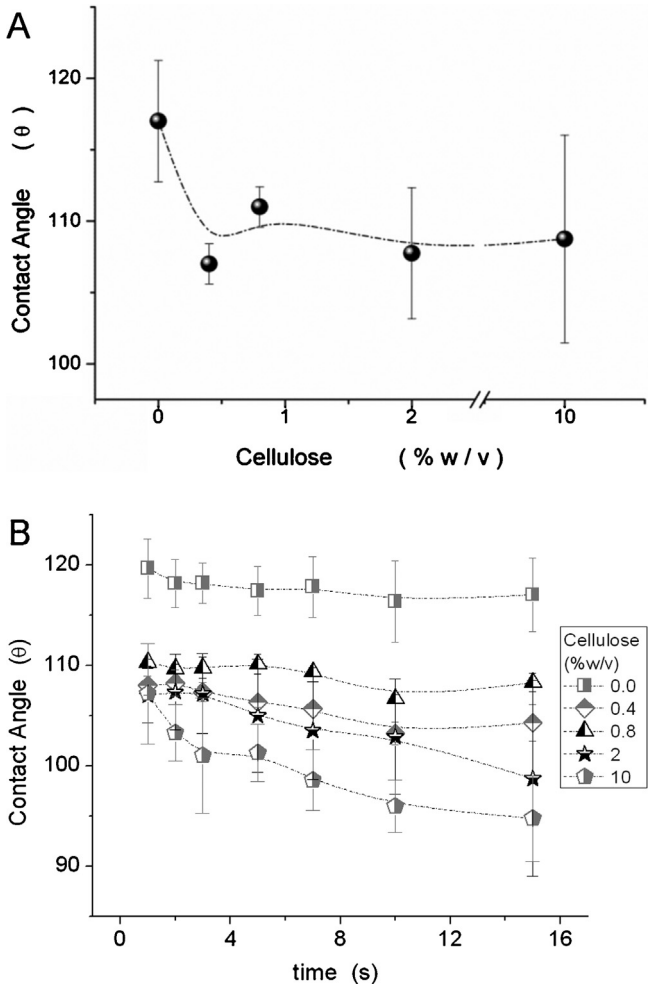

Fig. 2. (A) Contact angles (θ) of sessile drops of water after a contact of 1 s on p(MMA-NAT) 8-12 (B) contact angles (θ) of water on p(MMA-NAT) 8-12 (0, 0.4, 0.8, 2, 10% w/v cellulose content, respectively) versus time of contact of the drop on the polymer surface.

of 1 s on hydrogels containing 0, 0.4, 0.8, 2 and 10% w/v of cellulose. Hydrogels in the absence of cellulose had contact angles of $118 \pm 5°$; however, in the presence of cellulose, they decreased to 110° (average). These results indicate that the presence of cellulose slightly improves wettability.

Fig. 2B shows the kinetics of contact angle of water on samples with different cellulose content. All samples analyzed showed a decrease in the contact angle over time. Furthermore, the rate of decrease of contact angle increased at higher cellulose concentrations. These results indicate that the presence of cellulose in polymer composition improves wettability.

Subsequently, the equilibrium-swelling ratio (%ESR) of hydrogels was analyzed in the presence and absence of cellulose. As shown in Fig. 3, %ESR decreased with the percentage of cellulose from 370 to 254% for p(MMA-NAT) 8 and p(MMA-NAT) 12, respectively. The results indicate that the presence of cellulose favored interactions between polymer chains and therefore decreased interactions with water. However, the swelling should not decrease too much since it is required for switching the actuator. The %ESR decreased 22, 35, 37 and 116% on average for materials prepared with 0.4, 0.8, 2 and 10% w/v of cellulose, respectively. Therefore, the hydrogel containing 2% w/v of cellulose [p(MMA-NAT) 11] was selected since it was yielded in the higher concentration with a slight decrease in %ESR.

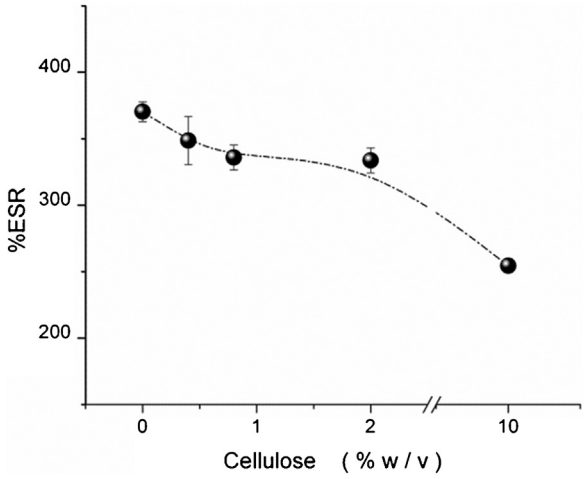

Fig. 3. Equilibrium swelling ratio (%ESR) of p(MMA-NAT) 8-12.

To verify the effect of cellulose addition, hydrogel samples were morphologically studied using an optical microscope at 5, 20 and 200× magnifications. Fig. 4 shows dry samples of hydrogels obtained in the absence [p(MMA-NAT) 8] and presence [p(MMA-NAT) 11] of 2% w/v cellulose. The hydrogel without cellulose (below) was glassy; yet, the presence of cellulose provided opacity and a whitish appearance (above). Furthermore, the gel without cellulose showed zones of macroscopic fractures and a rough appearance at 200×. When the cellulose-containing gel was dried, the fracture process did not occur. This improvement supports the use of cellulose fibers as reinforcing agents for the gel structure.

3.2. Characterization of cellulose-containing gels

Samples of dehydrated p(MMA-NAT) 11 were swelled in water and subsequently freeze-dried to retain their swollen structure. Fig. 5 shows SEM images of hydrogels without (A) and with (B) cellulose at 500×. The materials showed pores (A and B); however, porosity was lower when the hydrogel incorporated cellulose (B). Fig. 5B shows the presence of elongated fibrous structures distributed along the whole material. At a higher magnification (Fig. 5C), fibers are found to be easily distinguishable; however, few fibers are seen free, as shown in Fig. 5B, probably because cellulose is closely associated with the polymeric material.

To study the behavior of p(MMA-NAT) 11 in contact with water, hydrogel discs were dehydrated in the oven at 37 °C until constant weight, placed in water and rehydrated in order to measure mass change versus time. Fig. 6 shows swelling kinetics results. It can be observed that p(MMA-NAT) 11 incorporated water more rapidly in the first swelling phase until 90% SR. Then, the increase in water absorption was slight. In general, gels reached 50% of swelling equilibrium in approximately 130 min, while 99% of the final swelling was achieved at 24 h. The %ESR reached (330%, marked with a dash line in Fig. 6) was appropriate for using the material as an actuator.

The swelling kinetics was used to determine the type of mechanism of water diffusion within the hydrogels using Eq. (3). The diffusion law predicts that: if $0 < m < 0.5$, a Fickian diffusion mechanism controls water diffusion, whereas if $0.5 < m < 1$, the mechanism is not Fickian, whether $m = 1$ corresponds to a Type II mechanism [30]. The diffusion coefficient m was 0.31 ± 0.02, which corresponds to a Fickian mechanism. Therefore, the rate of diffusion is lower than the relaxation rate of polymeric chains.

To analyze the behavior of p(MMA-NAT) 11 in contact with soils with different water content, swelling equilibrium assays were developed. As indicated in the experimental section, the gels in dry

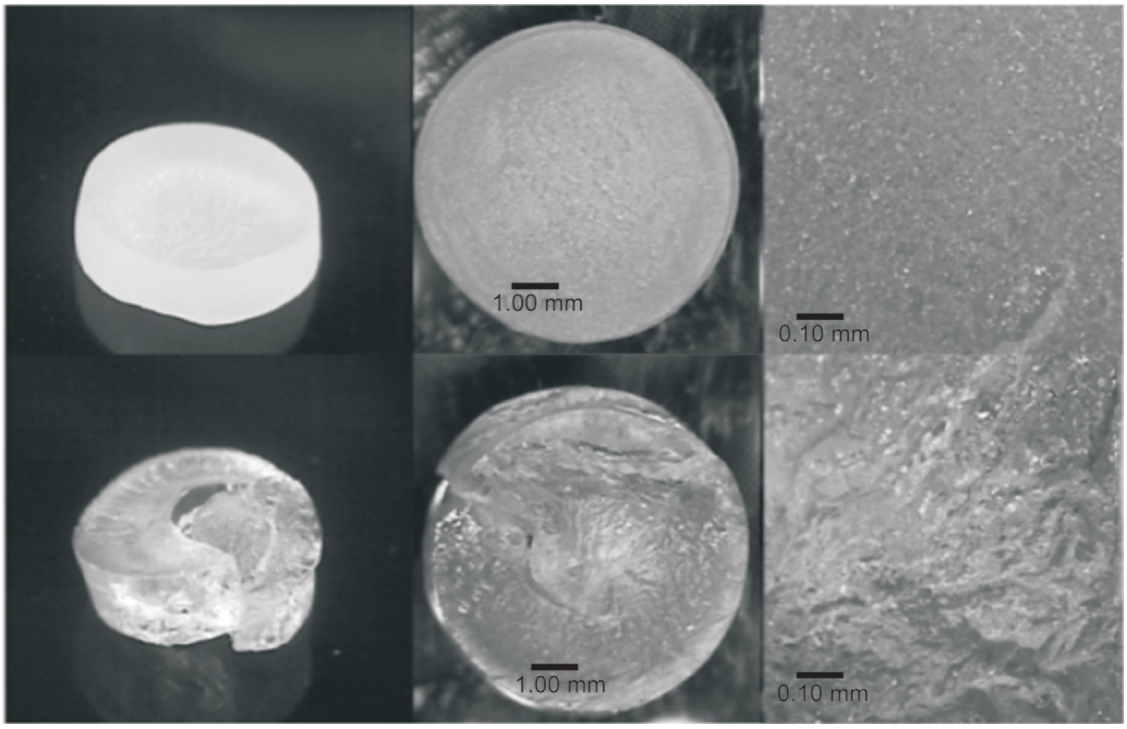

Fig. 4. Dried hydrogels with [up, p(MMA-NAT)11] and without [down, p(MMA-NAT)8] cellulose. From left to right: 5, 20, and 200× magnifications.

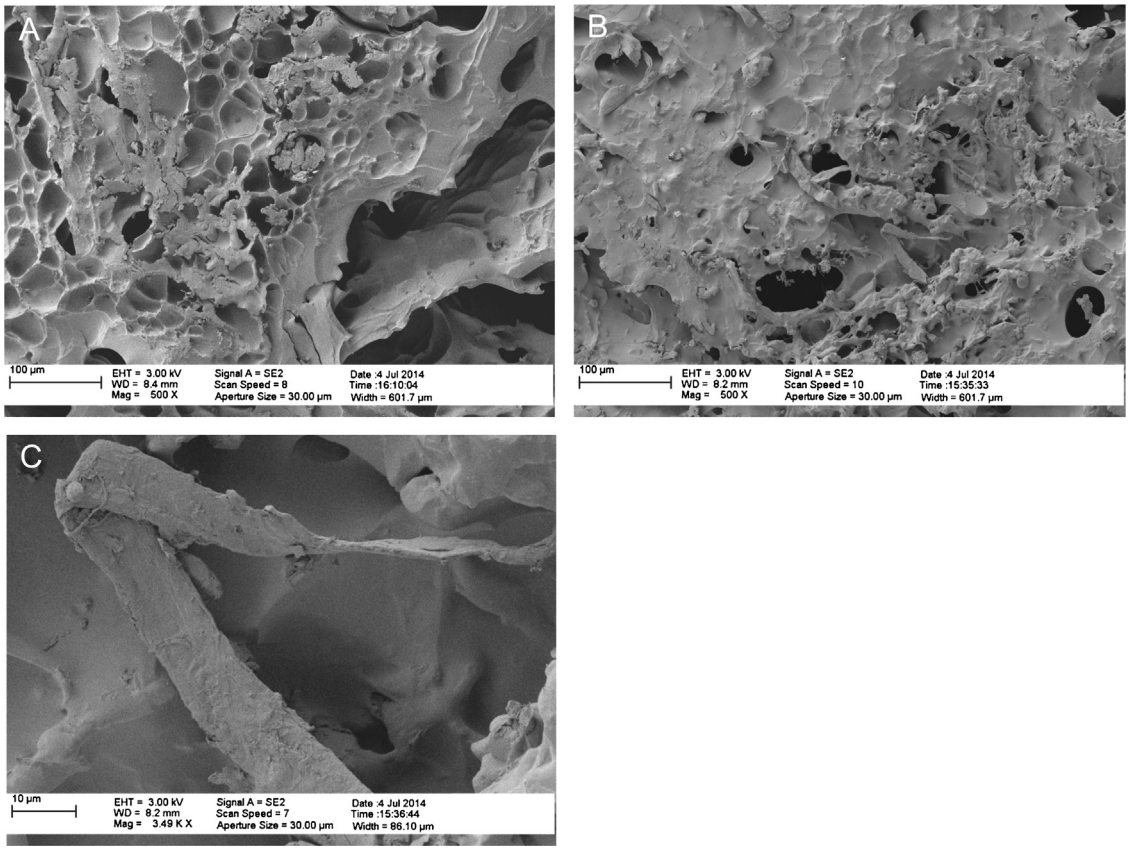

Fig. 5. SEM image of hydrogel with [A, p(MMA-NAT) 11] and without [B, p(MMA-NAT) 8] cellulose at 500×. (C) Hydrogel p(MMA-NAT) 11 at 3490×.

state were weighted and put in contact with different moisture content soils (0, 30, 45 and 60% v/v) in a closed system. For 5 days, the hydrogels were allowed to equilibrate with the environment and weighted after the test. As shown in Fig. 7, the gels swelled in proportion to the soil moisture up to 220 %ESR of its initial volume. Furthermore, this could be linearly extrapolated to the soil moisture of 100% (arrow). This correlated very well with the %ESR previously obtained in the test of swelling in water, shown in Fig. 6. Therefore,

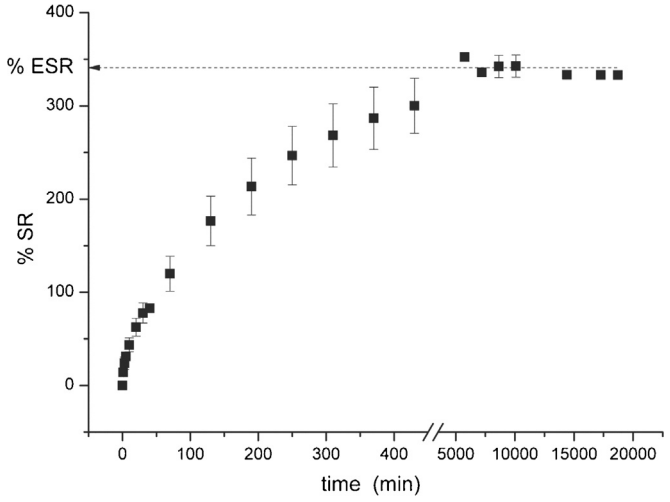

Fig. 6. Swelling kinetics of p(MMA-NAT) 11 and equilibrium swelling ratio (%ESR) reached (dash line).

the swelling of p(MMA-NAT) 11 was directly proportional to the moisture content of the environment.

NF kinetics was studied during the swelling of p(MMA-NAT) 11 hydrogels in water, using the methodology described in the experimental section. Fig. 8 shows the results of the force produced due to the expansion of the dehydrated hydrogel discs while absorbing water. NF significantly increased at the beginning of the test, probably due to the force produced by absorption of water from the surface of the polymer in dehydrated state. After a fast increase in strength, an inflexion was observed during the hydration process (Fig. 8, arrow). NF then continued growing with a slope lower than that of the initial increase, reaching 11 N (in the time measured).

The NF of p(MMA-NAT) 11 in contact with the ground at different moisture levels was evaluated. As explained in Materials and methods, the hydrogels were previously equilibrated on soils with different moisture content. Subsequently, the NF produced during

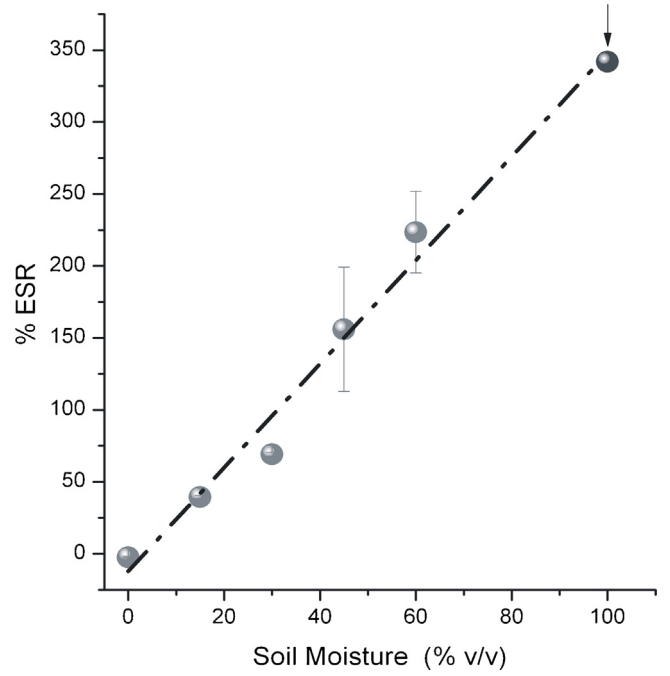

Fig. 7. Equilibrium swelling ratio (%ESR) vs. soil humidity for p(MMA-NAT) 11.

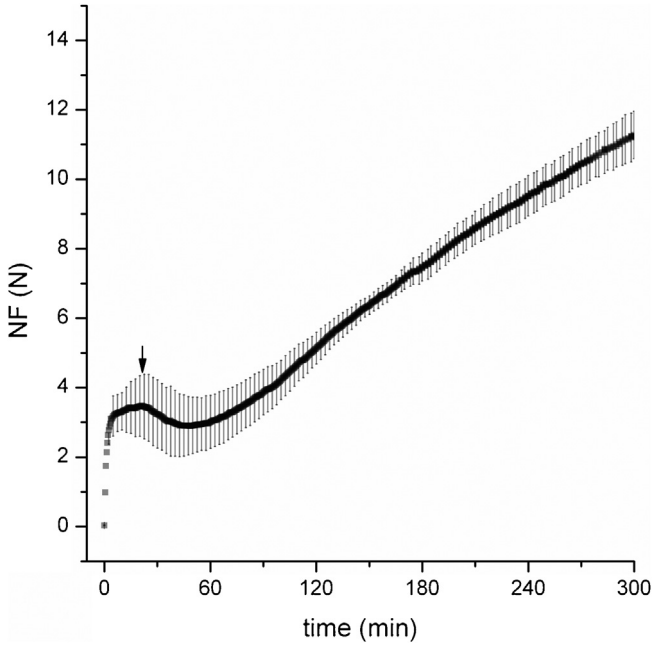

Fig. 8. Normal force (NF) vs. time for p(MMA-NAT) 11. The arrow shows an inflexion of the swelling force.

the swelling in water was measured. Fig. 9 shows equilibrium NF versus soil moisture content for p(MMA-NAT) 11. The NF decreased as moisture increased, and these variables are related in an approximately linear manner. The hydrogel was previously equilibrated in environments with different water content. Hence, the NF developed was a fraction of the total NF, because the network was already partially swollen. Therefore, the hydrogel inside the actuator could reach a high force when the soil is dry and a less force when soil humidity is raised.

The force produced by the actuator when a different moisture amount is present in the soil can be analyzed using the data from this graph. These results indicate that the hydrogels developed show swelling and expansion force closely associated with soil moisture and therefore this knowledge can be used in sensors or actuators to control water irrigation in the soil.

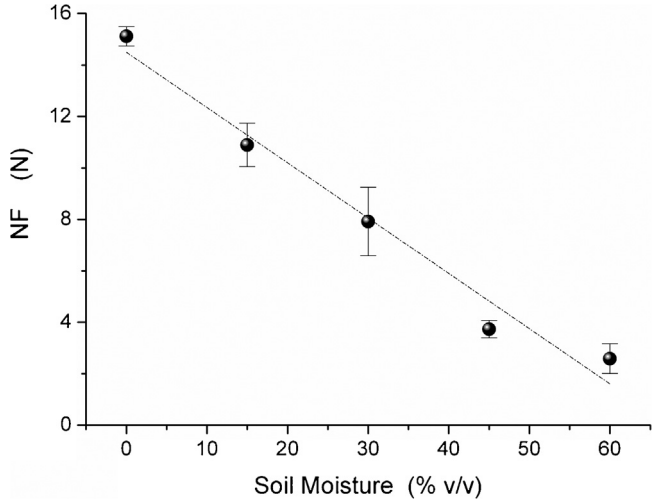

Fig. 9. Normal Force (NF) for p(MMA-NAT) 11 pre-equilibrated in soil with different moisture content (0; 15; 30; 45 and 60% v/v).

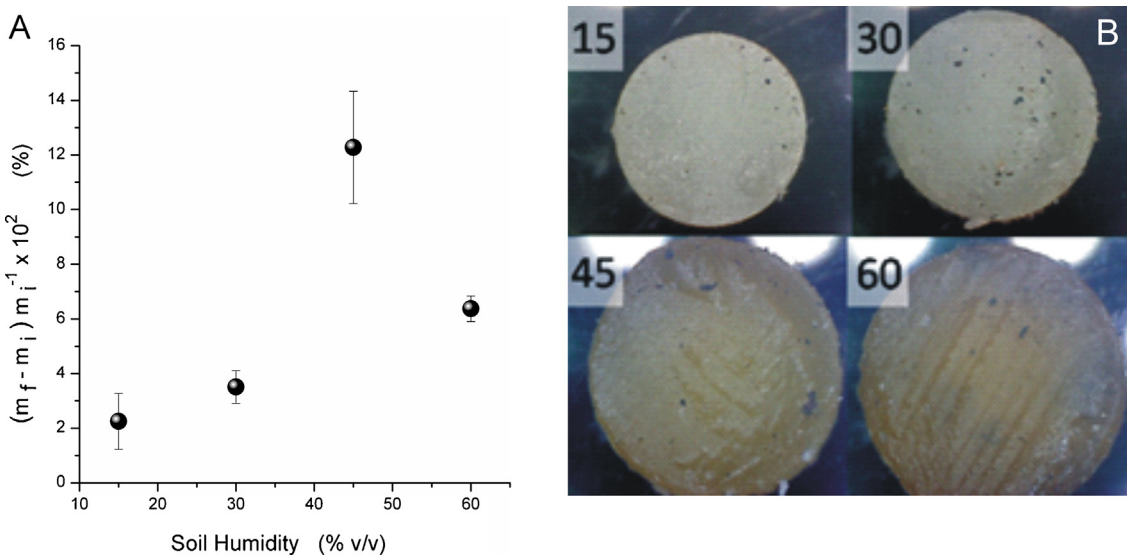

Fig. 10. (A) Variation of weight versus soil humidity for cellulose-containing hydrogels. (B) photos of the hydrogels swelled at equilibrium with soils at 15, 30, 45 and 60% H after 3 months.

3.3. Stability test for hydrogels in soil

Hydrogels containing cellulose were evaluated for 3 months in contact with soil of different humidity. The weight of the hydrogels before and after this period was determined. Fig. 10(A) shows the results. Weight variation was always positive as compared to that of the initial mass. This increase could be attributed to the retention of substances by soil. The maximum variation was 12.5% for the hydrogel equilibrated at 45% of humidity. However, it was observed that the mass increased only 6% when the hydrogel was in contact with soil at 60% of humidity. This effect could be due to polymer degradation at high humidity, favored by microbial activity. Furthermore, the soil equilibrated at high humidity after the assay showed the release of nauseating gases. Fig. 10(B) shows the photos of the equilibrated hydrogels with different humidity in soils for 3 months. After the test, the hydrogels were brown-colored, increasing in intensity with the humidity content of the soil tested. However, macroscopic changes were not observed in the mechanical properties because no disc was broken after the test. Therefore, following the test, a valve was built with the hydrogel pre-equilibrated at 60% of humidity. Differences were not found in the performance of the valve prepared with this material or valves prepared with hydrogels recently synthesized.

3.4. Development of irrigation valve and operational test

The performance of the valve prototype can be described as follows (Fig. 1): from a reservoir, the water (1) flows through the valve toward the ground (2). The hydrogel is in contact with the soil, absorbs water from it (3) and swells (4). The increase in the volume of hydrogel causes displacement of the plunger (5) which closes water flow. When the soil dries, water flows from the gel to the soil (6) and the volume of the polymer decreases (7). This reduction in volume decreases the force over the plunger and opens the passage of water until the soil reaches adequate humidity. This cycle of sensing humidity and irrigation control is continuously repeated.

To decide the appropriate size of the hydrogel, it should be noted that size is related to the expansion force and speed of the response of the system. Hydrogels of large area produce a great force (15 N, for a disc of 1 cm^2), while response speed depends on the diffusion rate of the water into the gel. The latter depends on the dimension of smaller size, either the diameter or thickness (δ) of the discs and of the diffusion coefficient of the water in the polymer (D). Then, with discs of small dimensions, fastest responses are reached. The value can be estimated by the following equation, where t is the time required for the diffusion of the solvent molecules through the polymer [31–33]:

$$\delta^2 \approx Dt \quad (5)$$

The thickness of the gel used for the valve (2 mm, dry) is similar to that used in the determination of the swelling kinetics (Fig. 6). Therefore, we expect that the response time of the hydrogel within the valve may correspond to that observed in this assay, reaching 90% of the swelling in about 6 h. Moreover, according to the previous paragraph, if the thickness of the gel decreases, the response time is accelerated. However, if the gel is too thin, thickness differences between swollen and dry states are small, and the mechanical valve system must be excessively precise, and therefore difficult to develop. The gel used in the valve in the dry state is 2 mm thick and its thickness on the state of high hydration is approximately 3.2 mm. Thus, according to humidity percentage values of 15, 30, 45 and 60%, we expect that the changes in thickness are about 2.3, 2.5, 2.7 and 2.9 mm, respectively. The force required to switch the valve depends on the pressure of the water that enters into the valve. For example, if the water pressure input to the system is 1 bar and is applied through the inlet duct having an area of 0.5 mm^2, water enters into the device with a force of 0.05 N. To develop this strength, a hydrogel disk of small area can be used, which spends less material. The force that can be applied by a hydrogel of 0.045 cm^2 is between 0.09 and 0.6 N, at 60% and 0% of humidity (%v/v), respectively. Therefore, this force is sufficient to switch the actuator.

The size of the hydrogel disc [p(MMA-NAT) 11] was 4 mm in diameter and 3.2 mm thick, at equilibrium swelling in water (near 2.4 mm diameter and 2.0 mm thick in dry state). The swollen hydrogel was incorporated into the valve as shown in Fig. 1. The valve was then connected to the water supply and the regulator (as indicated in the experimental section) was adjusted to select the close position (because the hydrogel was swollen). Subsequently, to check the correct operation of the valve, the hydrogel was dried with an air dryer across the porous stone. The drying process was evidenced when the valve was automatically opened (Fig. 11A). Furthermore, when the porous stone was hydrated with water for several hours (when the hydrogel was initially dry), the valve

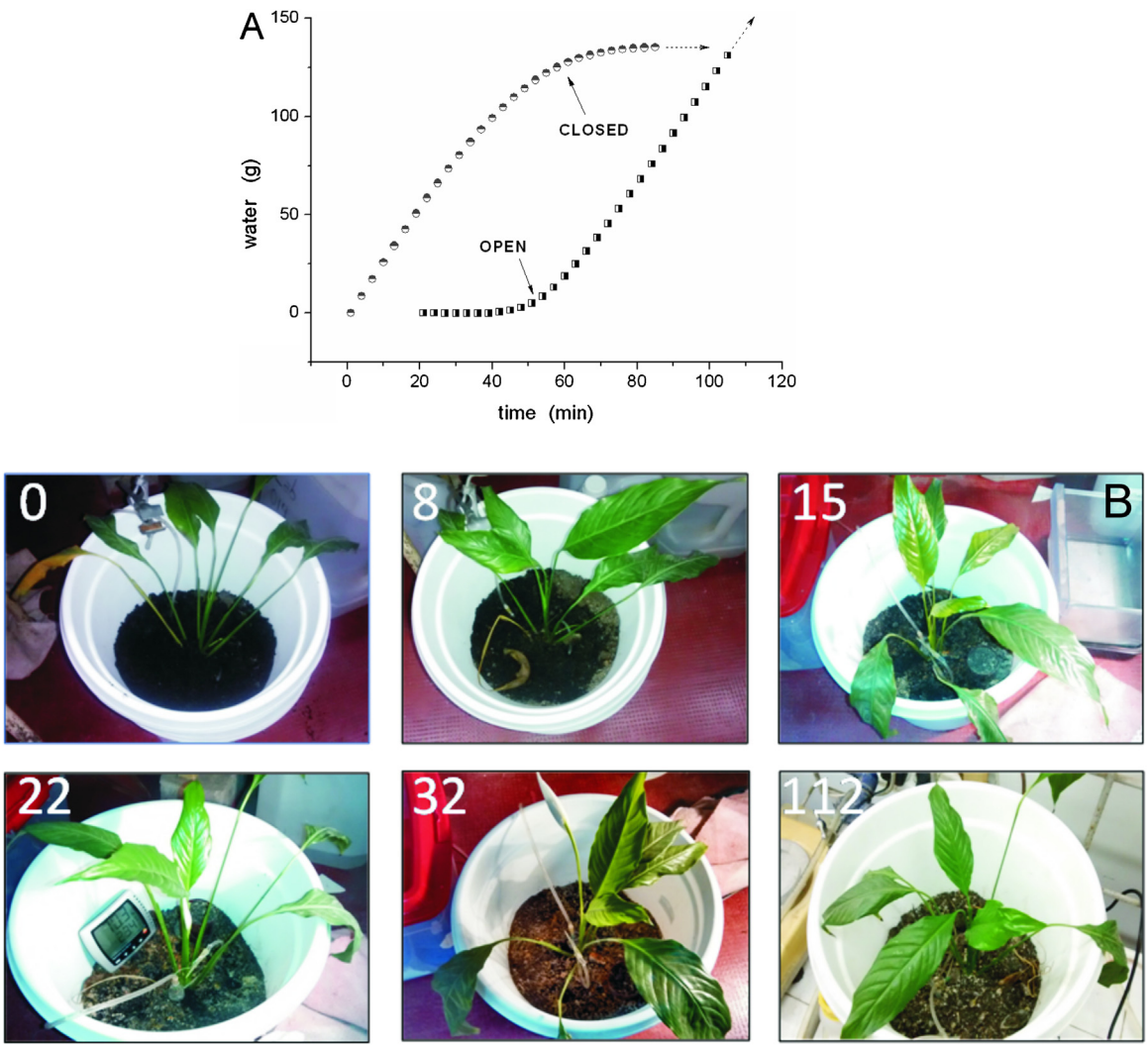

Fig. 11. (A) Mass of water flowing from the valve vs. time. The arrows show the autonomous process of opening and closing of the valve without being in contact with the soil; (B) photographic sequence at different days showing irrigation of the White calla lily plant in a pot, with the prototype valve as the only water supply.

automatically closed (Fig. 11A). The higher flux of water registered for this system was (8 ± 1) mL min^{-1} (measured with valves exposed to the air).

The automatic operation of self-regulation in contact with the soil was difficult to follow because of the long times needed to open and close. For this reason, the valve was evaluated for irrigation in a potted plant for a period of 4 months.

To evaluate the performance of the valve, it was placed on the ground, together with a *Zantedeschia aethiopica* plant (White calla lily) inside a plastic pot (Fig. 11). The valve was then connected to a water reservoir as indicated in the experimental section. The system thus set up was maintained at the laboratory for more than 100 days. During the period tested, the valve was observed to open and close and the plant was always kept in optimal conditions without morphological anomalies. Water consumption was approximately 3 L per month instead of about half a liter daily.

4. Conclusions

We developed an autonomous actuator capable of controlling soil moisture based on a selected hydrogel. In addition, this was developed at low costs considering that the system does not use electric power, as those of electronic type. Synthesized p(MMA-NAT) 11 hydrogel containing cellulose (2% w/v) showed adequate mechanical properties and all its characteristics were suitable to be used for developing a valve that controls water flow. The performance of the gel was evaluated with its swelling in different moisture content in soil. It was observed that the equilibrium swelling and expansion force reached were directly and inversely proportional to the amount of soil moisture, respectively, in the range studied. These results suggest that the hydrogel selected could be used as an actuator in the regulation of soil moisture. Subsequently, it was used to develop and operate a valve and control efficiently soil irrigation in a White calla lily plant. The response was very stable for more than 100 days. This system could be used to improve the management of water resources.

Acknowledgments

Authors acknowledge Consejo Nacional de Investigaciones Científicas y Técnicas (CONICET), Secretaría de Ciencia y Técnica de la Universidad Nacional de Córdoba (SECyT) and Fondo para la Investigación Científica y Tecnológica (FONCyT) for financial assistance. A. Wolfel also acknowledges receipt of fellowship from CONICET.

Appendix A. Supplementary data

Supplementary data associated with this article can be found, in the online version, at http://dx.doi.org/10.1016/j.snb.2016.04.104.

References

[1] X. Da-ping, G. Hong-yu, H. Dan, Discussion on the demand management of water resources, Procedia Environ. Sci. 10 (2011) 1173–1176.
[2] P. Belder, B.A.M. Boumana, R. Cabangon, L. Guoan, E.J.P. Quilang, L. Yuanhua, J.H.J. Spiertz, T.P. Tuong, Effect of water-saving irrigation on rice yield and water use in typical lowland conditions in Asia, Agric. Water Manage. 65 (2004) 193–210.
[3] L. Levidowa, D. Zaccaria, R. Maia, E. Vivas, M. Todorovic, A. Scardigno, Improving water-efficient irrigation: prospects and difficulties of innovative practices, Agric. Water Manage. 146 (2014) 84–94.
[4] M.D. Dukes, M. Shedd, B. Cardenas-Lailhacar, Smart Irrigation Controllers: How Do Soil Moisture Sensor (SMS) Irrigation Controllers Work? University of Florida, Institute of Food and Agricultural Sciences, FL, USA, 2009.
[5] M.D. Dukes, D.L. Bjorneberg, N.L. Klocke, Advances In irrigation: select works from the 2010 decennial irrigation symposium Am. Soc. Agric. Biol. Eng. 55 (2) (2012) 477–482.
[6] A.E. Caprio inventor and assignee. Differential relative humidity and temperature sensitive irrigation control. US patent 6585168 B1. 2003, July 1.
[7] J.E. Lattery, inventor; L. Parker assignee. Moisture sensing electronic irrigation control. US patent 5749521 A. 1998 May 12.
[8] T. Ojha, S. Misra, N.S. Raghuwanshi, Wireless sensor networks for agriculture: the state-of-the-art in practice and future challenges, Comput. Electron. Agric. 118 (2015) 66–84.
[9] R.W. Coates, M.J. Delwiche, A. Broad, M. Holler, Wireless sensor network with irrigation valve control, Comput. Electron. Agric. 96 (2013) 13–22.
[10] M. Dursun, S. Özden, An efficient improved photovoltaic irrigation system with artificial neural network based modeling of soil moisture distribution—a case study in Turkey, Comput. Electron. Agric. 102 (2014) 120–126.
[11] J.J. Cancela, M. Fandiño, B.J. Rey, E.M. Martínez, Automatic irrigation system based on dual crop coefficient, soil and plant water status for *Vitis vinifera* (cv. Godello and cv. Mencía), Agric. Water Manage. 151 (2015) 52–63.
[12] D.T. Eddington, D.J. Beebe, Flow control with hydrogels, Adv. Drug Deliv. Rev. 56 (2004) 199–210.
[13] K.W. Oh, C.H. Ahn, A review of microvalves, J. Micromech. Microeng. 16 (2006) 13–39.
[14] M.E. Harmon, M. Tang, C.W. Franka, A microfluidic actuator based on thermoresponsive hydrogels, Polymer 44 (2003) 4547–4556.
[15] J.B. Prettyman, D.T. Eddington, Leveraging stimuli responsive hydrogels for on/off control of mixing, Sens. Actuators B: Chem. 157 (2011) 722–726.
[16] D. Buengera, F. Topuza, J. Groll, Hydrogels in sensing applications, Prog. Polym. Sci. 37 (12) (2012) 1678–1719.
[17] M. Bassil, J. Davenas, M.E.L. Tahchi, Electrochemical properties and actuation mechanisms of polyacrylamide hydrogel for artificial muscle application, Sens. Actuators B: Chem. 134 (2) (2008) 496–501.
[18] H. Zhu, X. Zhou, F. Su, Y. Tian, S. Ashili, M.R. Holl, D.R. Meldrum, Micro—patterning and characterization of PHEMA-co-PAM-based optical chemical sensors for lab-on-a-chip applications, Sens. Actuators B: Chem. 173 (2012) 817–823.
[19] B.D. Johnson, D.J. Beebe, W.C. Crone, Effects of swelling on the mechanical properties of a pH-sensitive hydrogel for use in microfluidic devices, Mater. Sci. Eng. C 24 (2004) 575–581.
[20] M.R. Guilherme, A.V. Reis, S.H. Takahashi, A.F. Rubira, J.P.A. Feitosa, E.C. Muniz, Synthesis of a novel superabsorbent hydrogel by copolymerization of acrylamide and cashew gum modified with glycidyl methacrylate, Carbohydr. Polym. 61 (2005) 464–471.
[21] A. Sahoo, K.R.T. Ramasubramani, M. Jassal, A.K. Agrawal, Effect of copolymer architecture on the response of pH sensitive fibers based on acrylonitrile and acrylic acid, Eur. Polym. J. 43 (2007) 1065–1076.
[22] J.L. Holloway, A.M. Lowman, M.R. Van Landingham, G.R. Palmese, Interfacial optimization of fiber-reinforced hydrogel composites for soft fibrous tissue applications, Acta Biomater. 10 (2014) 3581–3589.
[23] C. Chang, L. Zhang, Cellulose-Based hydrogels: present status and application prospects, Carbohydr. Polym. 84 (2011) 40–53.
[24] S. Park, S.H. Kim, K. Won, J.W. Choi, Y.H. Kim, H.J. Kim, Y.H. Yang, H. Lee Sang, Wood mimetic hydrogel beads for enzyme immobilization, Carbohydr. Polym. 115 (2015) 223–229.
[25] S. Ito, M. Hashimoto, B. Wadgaonkar, N. Svizero, R.M. Carvalho, C. Yiu, F.A. Rueggeberg, S. Foulger, T. Saito, Y. Nishitani, M. Yoshiyama, F.R. Tay, D.H. Pashley, Effects of resin hydrophilicity on water sorption and changes in modulus of elasticity, Biomaterials 26 (2005) 6449–6459.
[26] I. Bravo-Osuna, C. Ferrero, M.R. Jiménez-Castellanos, Influence of moisture content on the mechanical properties of methyl methacrylate–starch copolymers, Eur. J. Pharm. Biopharm. 66 (2007) 63–72.
[27] M.R. Romero, R.D. Arrua, C.I. Alvarez Igarzabal, E.F. Hilder, Valve based on novel hydrogels: from synthesis to application, Sens. Actuators B: Chem. 188 (2013) 176–184.
[28] X. Zhang, Q. Wu, X. Li, S. Zheng, S. Wang, L. Guo, L. Zhang, J.B.M. Custers, Haploid plant production in *Zantedeschia aethiopica* 'Hong gan' using anther culture, Sci. Hortic. 129 (2011) 335–342.
[29] F. Ganji, S. Vasheghani-Farahani, E. Vasheghani-Farahani, Theoretical description of hydrogel swelling: a review, Iran. Polym. J. 19 (5) (2010) 375–398.
[30] A.S.T.M. International Standard Test Methods for Laboratory Determination of Water (Moisture) Content of Soil and Rock by Mass ASTM 2010 D2216-10 10.1520/D2216-10.
[31] A.J. Bard, L.R. Faulkner, Electrochemical Methods: Fundamentals and Applications, John Wiley, New York, 2001.
[32] W. Zhan, G.H. Seong, R.M. Crooks, Hydrogel-based microreactors as a functional component of microfluidic systems, Anal. Chem. 74 (2002) 4647–4652.
[33] F. Ganji, E. Vasheghani-Farahani, Hydrogels in controlled drug delivery systems, Iran. Polym. J. 18 (2009) 63–88.

Biographies

Marcelo Ricardo Romero, Doctor (Universidad Nacional de Córdoba, 2011). Currently he is an Assistant Professor at the Department of Organic Chemistry, School of Chemical Science, Universidad Nacional de Córdoba and Research Fellow of CONICET. His fields of interest include electrochemistry, analytical chemistry, polymer science, electronic devices, biosensors and actuators.

Alexis Wolfel, graduated from the Universidad Nacional de Córdoba where he obtained his Degree (2014). He is currently a Doctoral Fellow of CONICET in the Department of Organic Chemistry, School of Chemical Science, Universidad Nacional de Córdoba. His research interests are related with environmental sciences and shape memory polymers.

Cecilia Ines Alvarez Igarzabal, Doctor (Universidad Nacional de Córdoba, 1993). Currently she is a full Professor at the Department of Organic Chemistry, School of Chemical Science, Universidad Nacional de Córdoba and Research Fellow of CONICET, Argentina. Her fields of interest include synthesis, characterization and application of new polymeric materials and polymer science.